Direct observation of the ionization threshold of triplet methylene by photoionization mass spectrometry

Maritoni Litorja and Branko Ruscic
Chemistry Division, Argonne National Laboratory, Argonne, Illinois 60439-4831

(Received 31 December 1997; accepted 15 January 1998)

The photoionization spectrum of the ionization threshold region of methylene has been recorded for the first time. The CH_2 radical was produced *in situ* by successive hydrogen abstractions from methane precursor. The observed steplike onset corresponds to the vibrationless transition $CH_2^+\tilde{X}\ ^2A_1 \leftarrow CH_2\tilde{X}\ ^3B_1$ and leads to the adiabatic ionization energy of CH_2 of 10.393 ± 0.011 eV. This value is slightly higher than the nominal midrise of the threshold step structure, which is depressed by rotational autoionization effects. In a separate set of experiments, the threshold region of the CH_2^+ fragment from CH_3 was recorded at room temperature. The fragment appearance energy was accurately determined by fitting to be 15.120 ± 0.006 eV at 0 K. The combination of these two measurements provides the best current experimental value for the bond dissociation energy of the methyl radical, $D_0(\mathrm{H-CH_2}) = 4.727 \pm 0.012$ eV $= 109.0 \pm 0.3$ kcal/mol (corresponding to 110.4 ± 0.3 kcal/mol at 298 K), and yields $\Delta H_{f0}^{\ominus}(CH_2, \tilde{X}\ ^3B_1) = 93.2 \pm 0.3$ kcal/mol (93.3 ± 0.3 kcal/mol at 298 K) and $\Delta H_{f0}^{\ominus}(CH_2, \tilde{a}\ ^1A_2) = 102.2 \pm 0.3$ kcal/mol (102.3 ± 0.3 kcal/mol at 298 K). The latter makes the reaction $CH_2\ (\tilde{a}\ ^1A_2) + H_2O \rightarrow CH_3 + OH$ essentially thermoneutral, $\Delta H_{r0}^{\ominus} = 0.0 \pm 0.3$ kcal/mol. © *1998 American Institute of Physics.*
[S0021-9606(98)02715-9]

I. INTRODUCTION

In spite of numerous attempts, past efforts to determine directly the ionization energy (IE, or ionization potential) of methylene either by photoelectron spectroscopy or photoionization mass spectrometry have been frustrated by the difficulty of generating sufficient concentrations of this highly reactive radical. The only direct determinations of the IE are the relatively coarse measurements obtained early on by electron impact[1,2] (10.5 ± 0.2 and 10.35 ± 0.15 eV).

The best available value for the ionization energy of methylene, $\mathrm{IE}(CH_2) = 10.396 \pm 0.003$ eV, has been derived[3–5] by extrapolating the limit of the $nd\ ^3A_2$ Rydberg series from the first four members. Although computational theory can produce a ballpark value for $\mathrm{IE}(CH_2)$, it does not provide a particularly accurate audit of this quantity, since the calculated estimates typically differ by up to two-tenths of an eV.[6]

Considering the fact that methylene is a rather fundamental radical, it is quite surprising to see that its heat of formation has not yet been firmly and accurately established by experimental means. Wagman *et al.*[7] list $\Delta H_{f0}^{\ominus}(CH_2) = 93._2$ kcal/mol, supposedly superseded by the JANAF compilation,[8] which selects 92.2 ± 1.0 kcal/mol. On the other hand, Gurvich *et al.*[9] suggest 93.2 ± 1.0 kcal/mol, exactly 1 kcal/mol higher than JANAF,[8] and virtually identical to the older value by Wagman *et al.*[7]

In their recent review, Berkowitz *et al.*[10] avoid making a final recommendation for this quantity. However, in the section detailing photoionization results they list $D_0(\mathrm{H-CH_2}) = 108.2 \pm 0.7$ kcal/mol. This implies $\Delta H_{f0}^{\ominus}(CH_2) = 92.4 \pm 0.7$ kcal/mol, close to the JANAF value. The suggested bond energy was derived by Berkowitz *et al.* from a positive ion cycle involving the appearance energy (AE, or appearance potential) of the CH_2^+ fragment from CH_3 obtained by Chupka and Lifshitz[11] and the $\mathrm{IE}(CH_2)$ inferred by Herzberg.[4] This cycle, at least in principle, provides a very sound and straightforward thermochemical path to $D_0(\mathrm{H-CH_2})$ and hence $\Delta H_f^{\ominus}(CH_2)$. However, upon closer scrutiny, one finds that Chupka and Lifshitz[11] obtained $\mathrm{AE}_0(CH_2^+/CH_3) = 15.09 \pm 0.03$ eV using a fairly unusual procedure. They examined the CH_2^+ fragmentation onset from CH_3 at several temperatures in the 810–1110 K range. After a detailed analysis of the data, the authors concluded that, as a consequence of subsequent collisions, the actual temperature of the CH_3 radical in the ionization region is considerably lower than the measured temperature of their pyrolytic source. Hence, they rejected the customary threshold extrapolation method (which would require a reasonably accurate knowledge of the sample temperature) in favor of an inventive but difficult approach that makes use of the inflection point at the foot of the fragment yield curve. Such point, where the true fragment onset merges with the exponential tail extending to lower energies, indeed corresponds directly to the 0 K fragment appearance energy. However, in practice this is very rarely exploited because locating the desired feature of the fragment yield curve with any degree of certainty proves to be extremely difficult.

Other positive ion cycles potentially useful in determining $\Delta H_f^{\ominus}(CH_2)$, which were presumably considered by Berkowitz *et al.*[10] and discarded as less reliable, involve photoionization measurements of the CH_2^+ fragment onset either from methane[12–14] or ketene.[14] Although there are recent indications[15] that these determinations may be some-

what off, the onset of CH_2^+ from ketene, as determined by McCulloh and Dibeler,[14] is $AE_0(CH_2^+/CH_2CO) = 13.729 \pm 0.008$ eV. This implies $D_0(H_2C{=}CO) = 76.9 \pm 0.2$ kcal/mol, and with[16] $\Delta H_{f0}^{\ominus}(CH_2CO) = -10.7 \pm 0.4$ kcal/mol, leads to $\Delta H_{f0}^{\ominus}(CH_2) = 93.4 \pm 0.4$ kcal/mol. Using $AE(CH_2^+/CH_4)$ would appear to have the advantage of tying the heat of formation of methylene directly to that of methane, rather than ketene. Unfortunately, the underlying fragmentation process cannot be realistically expected to yield a thermochemically reliable threshold. The lowest channel generating the CH_2^+ fragment from methane corresponds to a sterically unfavorable H_2 elimination, which must compete with the simple bond breakage to $CH_3^+ + H$ that occurs at lower energy. Such a situation is prone to a ''kinetic shift'' in the appearance energy. Hence, the measured onset is likely to provide only an upper limit, such as[13] $\Delta H_{f0}^{\ominus}(CH_2) \leqslant 94.6 \pm 0.5$ kcal/mol, or perhaps[14] even as low as $\leqslant 93.8 \pm 0.5$ kcal/mol.

Two very frequently cited experimental sources[17,18] of $\Delta H_f^{\ominus}(CH_2)$ are based on measurements of the photodissociation of ketene yielding singlet methylene. The 0 K threshold values for this process deduced by the two studies are very similar: 85.2 ± 0.3 and 85.4 ± 0.3 kcal/mol. With the precisely known value[19] for the $\tilde{a}\,^1A_1 - \tilde{X}\,^3B_1$ separation in CH_2, 3156 ± 5 cm^{-1} (9.023 ± 0.014 kcal/mol), the two thresholds yield an average of $D_0(H_2C{=}CO) = 76.3 \pm 0.3$ kcal/mol implying $\Delta H_{f0}^{\ominus}(CH_2) = 92.8 \pm 0.6$ kcal/mol. On the other hand, Hayden *et al.*[20] measured $77.6(\pm 0.6)$ kcal/mol for the dissociation of ketene to triplet methylene and 86.1 ± 0.5 kcal/mol to singlet methylene. These determinations imply a significantly different value of $\Delta H_{f0}^{\ominus}(CH_2) = 93.9 \pm 0.7$ kcal/mol.

Not surprisingly, the literature abounds with theoretical attempts to determine $\Delta H_{f0}^{\ominus}(CH_2)$. At the standard GAUSSIAN-2 (G2) level,[21] *ab initio* theory yields 94.6 kcal/mol, higher than most experimental values. Recently, Grev and Schaefer[22] performed a particularly careful systematic study of correlation effects and other corrections using large atomic natural orbital basis sets and coupled cluster methods including single, double, and triple excitations [CCSD(T)]. They found the upper and lower limits of 92.8 kcal/mol $\leqslant \Delta H_{f0}^{\ominus}(CH_2) \leqslant 94.1$ kcal/mol, and extrapolated $\Delta H_{f0}^{\ominus}(CH_2) = 93.4 \pm 0.5$ kcal/mol. Very recently, Peterson and Dunning[23] performed a different study using systematic sequences of correlation consistent basis sets and carried out their calculations at various levels of theory including CCSD(T) and several multireference configuration interaction methods. Their calculated $D_e(H{-}CH_2) = 116.9$ kcal/mol translates to $D_0(H{-}CH_2) = 108.9$ kcal/mol, and implies $\Delta H_{f0}^{\ominus}(CH_2) = 93.1$ kcal/mol. Using correlation consistent polarized core-valence basis sets at the CCSD(T) level, Doltsinis and Knowles[24] attempted another approach to estimate various corrections. They extrapolated 92.9 ± 0.2 kcal/mol, and noted that a more accurate experimental determination of $\Delta H_f^{\ominus}(CH_2)$ is urgently required.

We have recently[25] reported on a photoionization investigation of CH_3 equilibrated at room temperature. The radical was generated *in situ* by hydrogen abstraction from methane. The study had a twofold purpose: It has demonstrated that the shape and apparent location of the ionization threshold region of CH_3 is influenced by rotational autoionization, and, with the aid of a carefully redetermined appearance energy of CH_3^+ from CH_4, it has produced a tuned-up value of $D_0(H{-}CH_3)$ and hence $\Delta H_f^{\ominus}(CH_3)$.

In this paper we report on the related, but significantly more challenging (at least from the experimental viewpoint) study of the methylene radical. Methylene was prepared by two sequential hydrogen abstractions from methane. The approach provides sufficiently high concentrations of CH_2 to produce a photoionization spectrum of the threshold region and thus for the first time tests by direct observation the validity of Herzberg's[4] value for $IE(CH_2)$. In addition, the fragmentation threshold of CH_2^+ from CH_3 was examined at room temperature. With the aid of recently developed fitting procedures,[26] this measurement yields an accurate value for $AE_0(CH_2^+/CH_3)$. Together, $IE(CH_2)$ and $AE_0(CH_2^+/CH_3)$ provide the best currently available experimental determination of $D_0(H{-}CH_2)$, and hence, by virtue of the accurately known[10,25] value of $\Delta H_f^{\ominus}(CH_3)$, furnish a significantly improved value for $\Delta H_f^{\ominus}(CH_2)$.

II. EXPERIMENT

The basic instrumental setup employed in the present studies was recently described elsewhere.[26(g)] During experiments that utilized the many-lined Werner and Lyman emission bands of molecular hydrogen, the lines themselves provided an accurate[27(a)] internal wavelength calibration. In the case of the helium Hopfield emission continuum, the superimposed Ne I, N II, and H I atomic emission lines[27(b)] served the same purpose.

Both CH_3 and CH_2 were produced using *in situ* techniques. Fluorine atoms were generated in a low-pressure microwave discharge through pure fluorine and piped into a small cuplike region, where they reacted with the methane precursor. The construction of the radical source is such that species emanating into the ionization region have typically undergone several collisions with the source walls and are thus reasonably well equilibrated to ambient temperature. Methyl radical was generated by direct hydrogen abstraction from methane, while methylene radical was produced by driving the reaction a step further and abstracting a hydrogen from CH_3. It is suspected that the overall rate of the latter step was aided by reactions occurring on the walls of the radical source. The reaction yields of CH_3 and CH_2 were optimized by manually adjusting the output power of the microwave source and the flows of fluorine and methane. The CH_3 signal usually maximized at high to medium CH_4/F_2 flow ratios and, with some experience, it was possible to rather reproducibly find conditions yielding a stable concentration of the methyl radical with a very good signal to noise ratio. Not surprisingly, satisfactory production of CH_2 by successive abstractions was significantly more difficult to accomplish. In order to start converting a portion of CH_3 into CH_2, it was usually necessary to shift the reactant flows into a domain of low CH_4/F_2 ratios, which typically had a tendency to generate unacceptably high background

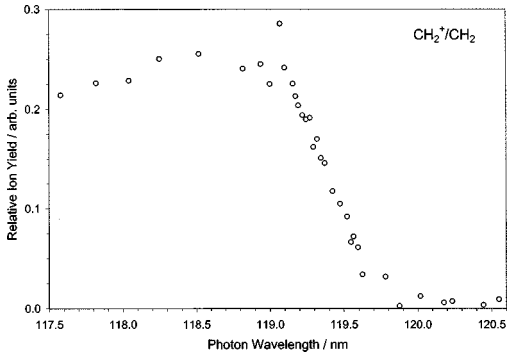

FIG. 1. The threshold region of the photoion yield curve of CH_2. Methylene radical was produced *in situ* by two successive hydrogen abstractions from methane. The radical is equilibrated at room temperature.

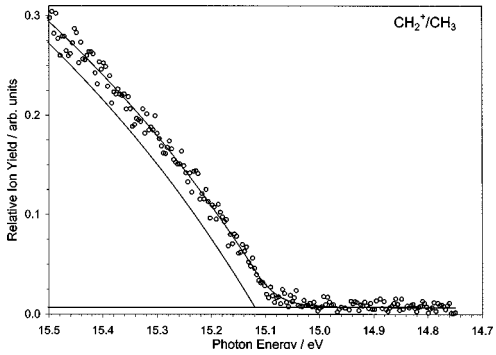

FIG. 2. The photoion yield curve of the CH_2^+ fragment from methyl radical. The solid line under the experimental points is a model fit at room temperature, while the line displaced toward higher energy is the derived fragment ion yield at 0 K. The fitted value for the appearance energy is $AE_0(CH_2^+/CH_3)=15.120\pm0.006$ eV at 0 K.

signals. However, depending on the status of the surfaces in the radical source, it was possible to gradually adjust the settings and obtain favorable experimental conditions of sufficiently high concentrations of CH_2 and reasonably low background, allowing the measurements presented here.

III. RESULTS

A. Parent ionization of CH_2

Figure 1 displays a mass-resolved ($m/z=14$) spectrum of the threshold region of CH_2 covering 117.5–120.6 nm. In order to achieve the best signal to noise ratio, the points have been recorded only at peak light intensities of the H_2 emission bands. The nominal spectral resolution was 0.08 nm. The wavelength scale calibration is believed to be correct to $\sim$0.05 nm. The raw spectrum of CH_2 had a minor contribution from the substantially stronger signal produced by parent ionization of CH_3. This contribution was completely attributable to incomplete mass separation of the quadrupole filter, causing about 0.5% of the ion intensity at $m/z=15$ to ''leak'' into $m/z=14$. This was established in separate experiments, which have also shown that the interfering CH_3 ion yield is relatively level and featureless in this region. Hence, within the statistical scatter of the data, the principal effect of the mass ''contamination'' was to generate a baseline offset.

The overall shape of the CH_2 ionization threshold shown in Fig. 1 is that of a prominent step, and corresponds to the vibrationless $(0\leftarrow0)CH_2^+\tilde{X}\ ^2A_1\leftarrow CH_2\tilde{X}\ ^3B_1$ transition. The nominal midrise position is at $\sim119.42\pm0.07$ nm$\equiv$10.382 ±0.006 eV, at an energy somewhat lower than the expected adiabatic IE. In the plateau region that appears at the short wavelength end, the sporadic data points hint to the existence of autoionization structure converging to higher vibrational levels of the ion.

It is interesting to note that the spectrum does not display discernible evidence of step structure corresponding to allowed excitations of totally symmetric vibrations of the ion. While $v'=1$ of the a_1 stretch (ν_1) is expected at energies higher than those covered by Fig. 1, the first quantum of the a_1 bend (ν_2) of $CH_2^+\tilde{X}\ ^2A_1$ should still fall within the examined region. Within the statistical significance of the data and potential masking effects of the autoionization structure in the plateau region, the Franck–Condon factor for $v'=1$ of ν_2 bend appears to be $<10\%$ (and probably significantly less) than the Franck–Condon factor for the $0\leftarrow0$ transition. Hence, the spectrum suggests that there is relatively little change in the HCH angle in going from $CH_2\tilde{X}\ ^3B_1$ to $CH_2^+\tilde{X}\ ^2A_1$. This leads to the inference that there is very little overall change in structure, since a significant change in the C–H bond length, which would lead to excitation of ν_1, would almost certainly be accompanied by a change in the HCH angle and a concomitant excitation in ν_2. Thus, even without explicit knowledge of the higher energy region of the spectrum, it can be concluded that the ionization onset of CH_2 is dominated by a very strong Franck–Condon factor for the $0\leftarrow0$ transition. Consequently, the vertical IE (defined as the highest vibrational peak in the photoelectron spectrum) and the adiabatic IE of CH_2 are the same. The inferred similarity of geometries of $CH_2\tilde{X}\ ^3B_1$ and $CH_2^+\tilde{X}\ ^2A_1$ is fully upheld by existing spectroscopic and theoretical studies.[5,6,22,23,28]

Within the small uncertainty of the correction for the mass ''leak'' discussed above, the spectrum in Fig. 1 shows no evidence of ionization from $CH_2\tilde{a}\ ^1A_1$. In principle, if ionization from singlet methylene were sufficiently strong, it should appear as a ''hot band'' extending $\sim$0.391 eV below the nominal ionization threshold for triplet methylene. Hydrogen abstraction by fluorine atoms from CH_3 is certainly sufficiently exothermic to produce methylene in the singlet state. Of course, if the nascent singlet–triplet distribution of the radical were to be efficiently relaxed by wall collisions in the source and hence equilibrated to room temperature, the resulting Boltzmann population of the singlet would be too small to observe experimentally. On the other hand, previous experience[29] appears to leave some quandaries on the efficiency of collisions in relaxing excited electronic states across different multiplicities. However, since most singlet methylene reactions proceed at collision rates,[30] it is very likely that the population of $CH_2\tilde{a}\ ^1A_1$ is depleted relative to $\tilde{X}\ ^3B_1$ primarily by the scavenging action of reactive wall collisions, rather than by relaxation.

B. CH_2^+ fragment from CH_3

Figure 2 displays the threshold region of the CH_2^+ fragment from CH_3, scanned at 0.02 nm point density. The nominal spectral resolution was 0.08 nm, while the absolute wavelength scale is correct to better than 0.02 nm. Under the conditions used to maximize the production of the CH_3 radical, contribution from parent ionization of CH_2 was completely negligible. However, the raw data contained a significant contribution from concomitant CH_2^+ fragmentation from unreacted CH_4, amounting roughly to 1/3 of the total signal on $m/z=14$ at $\sim$15.5 eV. This interference was easily corrected for by subtracting a separately recorded fragment ion yield curve of CH_2^+ from CH_4. The exact amount of correction was established by discharge on/off measurements at selected wavelengths prior and immediately after the runs, thus providing an accurate measure of the relative intensities of the two processes. A direct comparison of the two spectra (CH_2^+ from CH_4 and CH_2^+ from CH_3), when normalized to the same intensity at $\sim$15.5 eV, indicates that the threshold of CH_2^+ from CH_4 approaches the background level in a more curved fashion and appears at slightly higher energies[31] than that of CH_2^+ from CH_3. This fortuitous circumstance helps significantly in minimizing the influence of slight experimental imperfections likely to be present in the subtraction procedure. By varying the subtracted amount within the extremes that clearly yield undercorrected or overcorrected spectra, it was established that even under a pessimistic scenario the uncertainty in the AE arising from imperfect subtraction is relatively small (<0.003 eV), and contributes only trivially to the overall error bar.

The general shape of the curve in Fig. 2 is very reminiscent[25] of the ion yield of the CH_2^+ fragment from CH_4. In both cases the examined process proceeds via simple bond scission and corresponds to the energetically most favored fragmentation. Although in the present spectrum the experimental scatter is understandably larger, it can be clearly seen that the ion yield curve has a gentle convex overall curvature. Hence, this is another case where a traditional linear extrapolation to obtain AE_{298} could yield problematic results.

The procedure for obtaining appearance energies by fitting the experimental ion yield curves was described in detail previously.[26] The line passing through the data in Fig. 2 is a least-squares fit with a threshold model function, while the line displaced toward higher energy is the implied hypothetical fragment ion yield at 0 K. The kernel function used here was of the form $\{1-\exp[-B(h\nu-E_T)]\}$, and the internal energy distribution function had the form $E^{\eta}\exp(-aE)$, where $h\nu$ is the photon energy, E_T is the fragmentation threshold, and B, η, and a are adjustable parameters. Parameter η of the function representing the internal energy distribution of CH_3 was predetermined with the aid of Haarhoff's expression[32] for the density of states, which was computed numerically in the range of interest using tabulated[33] vibrational frequencies. Parameter a was obtained by imposing the requirement that the overall function reproduces the correct amount of average internal energy available for fragmentation at 298 K (0.0432 eV).

The overall quality of the fit in Fig. 2 is very satisfactory, and produces $AE_0(CH_2^+/CH_3)=15.120\pm0.006$ eV (15.077 eV at 298 K). This is nominally higher, although still barely within the coarser experimental error bar of the previous[11] value (15.09 ± 0.03 eV), which was obtained from hot CH_3 as discussed in Sec. I.

IV. DISCUSSION

A. IE(CH_2) and rotational autoionization in the threshold region

The nominal midrise of the threshold step in Fig. 1 is slightly lower ($\sim0.014\pm0.007$ eV) than the adiabatic ionization threshold derived by Herzberg.[4] In principle, it is possible that the extrapolated ionization limit is not entirely correct,[34] since it is based on a very short Rydberg series. On the other hand, as shown recently[25] for CH_3, the apparent midrise of the steplike shape may be depressed if rotational autoionization is a significant contributor to the overall ionization process in the threshold region.

The configuration of CH_2 in its ground state is $(1a_1)^2(2a_1)^2(1b_2)^2(3a_1)^1(1b_1)^1\ ^3B_1$. The lowest state of the CH_2^+ ion, $\tilde{X}\ ^2A_1$ is generated by the $(1b_1)^{-1}$ ionization process. The dipole-allowed ionization continua accessible from the ground state of CH_2 have overall symmetries of $^3A_1$, $^3A_2$, and $^3B_1$, and can be formed by coupling $ks\ a_1$, $kd\ a_1$, $kd\ a_2$ and $kd\ b_1$ outgoing waves with the $CH_2^+\tilde{X}\ ^2A_1$ ion core. In the discrete region, these four ionization continua correlate with the analogous dipole-allowed Rydberg series: $[^2A_1]ns\ ^3A_1$, $[^2A_1]nd\ ^3A_1$, $[^2A_1]nd\ ^3A_2$, and $[^2A_1]nd\ ^3B_1$. Unfortunately, not much is known about these Rydberg states. Herzberg[3] observed at 141.5 nm a band possessing very simple rotational structure (P and R branch only, with prominent even–odd intensity alternation). The striking similarity to a $\Sigma\leftarrow\Sigma$ band led initially to an interpretation within a framework of a supposedly linear CH_2. Later, when it became clear that $CH_2\tilde{X}\ ^3B_1$ is bent,[28] the transition was reinterpreted[5,35] as the $K'=0\leftarrow K''=0$ subband of $\tilde{B}(3d)^3A_2\leftarrow\tilde{X}\ ^3B_1$. In a paper[4] following the initial reports on CH_2, Herzberg identified three additional members ($n=4-6$) of the same series, providing the basis for the extrapolated IE(CH_2). In addition to the $nd\ ^3A_2$ series, Herzberg reported[3] on two ''strong line-like features,'' at 141.01 and 139.68 nm. These were interpreted as Q branches corresponding to 0–0 vibrational bands of electronic transitions to the other two $3d$ Rydberg states ($\tilde{C}$ and $\tilde{D}$). Tentatively, Herzberg also suggested[3] that a ''weak band'' at 169.0 nm could correspond to the $3s$ Rydberg state. The existence and the approximate location of all three $3d$ ($\tilde{B}$, $\tilde{C}$, and $\tilde{D}$) as well as one $4d$ state in methylene has been confirmed recently using resonantly enhanced multiphoton ionization (REMPI) techniques.[36]

In order to assess the possible influence of rotational autoionization, one has to briefly examine the relevant rotational structure. Both CH_2 and CH_2^+ in their ground states are slightly asymmetric (almost prolate) tops.[33,37,38] The twofold axis of the C_{2v} molecular group coincides with the inertial b axis, while the c axis is perpendicular to the molecular plane. The rotational levels can be conveniently classified using the

$N_{K_aK_c}$ notation, where N is the total angular momentum apart from spin and K_a and K_c are the quantum numbers of rotation about the a and c axes.[39] The rotational levels can be organized into stacks having a common value for K_a, and $N=K_a$, K_a+1, K_a+2, etc. In the $K_a=0$ stack, K_c is restricted to $K_c=N$. For $K_a>0$, each K_a value generates two nearly degenerate stacks, corresponding to $K_c=(N-K_a)$ and $K_c=(N-K_a)+1$. Each level can also be tagged with Dennison-type labels ($++$, $+-$, etc.) reflecting the symmetry behavior of the rotational function with respect to rotation about the c and a axes. Within a single stack, the labels oscillate between two alternatives ($++/-+$ or $+-/--$). Since CH_2 has two identical H nuclei, the alternation between Dennison labels correlates with the overall symmetric or antisymmetric classification, with an associated 3:1 alternation in statistical weight. The nearly degenerate pairs of levels across two stacks with same K_a have complementary Dennison labels, and consequently produce symmetric/antisymmetric pairs. Since the difference between rotational constants B and C is relatively small, the energy of the rotational levels can be approximated sufficiently well (at least for the purpose at hand) using the symmetric top formula with K_a having the role of K.

An approximation to the relevant rotational structure was generated using known rotational constants[33,37,38] of CH_2 and CH_2^+. The individual line intensities were estimated by taking into account nuclear spin statistics, degeneracy, and the Boltzmann population of the initial states, as well as the nuclear spin statistics and degeneracy of the ionic states. The straightforward application of standard selection rules,[39(b)] $\Delta N=0$, ± 1, and $\Delta K_a/\Delta K_c=$even/odd ($^3A_2 \leftarrow {}^3B_1$), odd/even ($^3A_1 \leftarrow {}^3B_1$), or odd/odd ($^3B_1 \leftarrow {}^3B_1$), yields three primary branches (P, Q, and R) with a large number of possible subbranches. It is almost certain that not all possible subbranches will be equally important in ionization or absorption to discrete Rydberg states. In the absence of a rotationally resolved photoelectron [i.e., zero electron kinetic energy (ZEKE)] spectrum, further clues on the importance of various branches and subbranches can be obtained from the behavior in the discrete region. In particular, Herzberg has shown[3] that $3d\ {}^3A_2 \leftarrow \tilde{X}\ {}^3B_1$ does not display a Q branch. This can be rationalized by assuming that only $\Delta K_a=0$ is important. Furthermore, the strong even/odd alternation of observed line intensities[3] suggests that only transitions originating from the $K_a=0$ stack are significant, since the inclusion of higher K_a stacks would quickly dilute the intensity alternation. For lack of better indicators, it can be assumed that ionization to the $kd\ {}^3A_2$ continuum will parallel this behavior. What exactly has to be included to simulate ionization to the $ks/kd\ {}^3A_1$ and $kd\ {}^3B_1$ continua is somewhat less clear. The two related $3d$ Rydberg states appear[3] as rather strong Q-like (i.e., compact) branches. Here $\Delta K_a=0$ is not possible, since selection rules dictate that ΔK_a be odd. The change in K_a makes the subbranches corresponding to $\Delta N=0$ spread out, and hence the features observed by Herzberg[3] are probably not real Q branches. However, other subbranches produce compact Q-like features. In particular, the $\Delta N=-1, K_a'=1 \leftarrow K_a''=0$ subbranch is quite compact, both in the case of $^3A_1$ and $^3B_1$ final states. Hence, one could assume that ionization to $kd\ {}^3A_1$ and $^3B_1$ continua can be fairly represented by including such a branch. The relative intensity of the Q-like feature relative to the P and R branches of the $kd\ {}^3A_2$ continuum is less clear. Also, since ns Rydberg states have not been positively identified in the discrete region, it is not clear how important transitions are to the $ks\ {}^3A_1$ continuum.

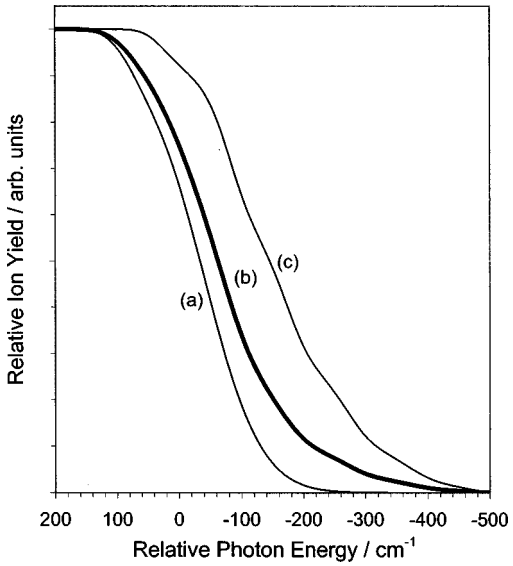

FIG. 3. Illustration of the effect of rotational autoionization in the ionization threshold region of methylene. The abscissa is relative to the adiabatic ionization energy. (a) Curve incorporating only direct ionization. (b) Curve incorporating rotational autoionization by loss of two rotational quanta of the core, $\Delta N=-2$, without allowing interactions across different K_a stacks. (c) Curve providing an upper limit to the effect by incorporating rotational autoionization by $\Delta N=-1,-2$ of all Rydberg states that are sufficiently energetic.

However, for the simple purpose of assessing the importance of rotational autoionization in the context of a rotationally unresolved photoionization spectrum, it is not unreasonable to accept the provisions outlined above. Hence, the model assumes that the bulk of the underlying rotational structure of the ionization threshold can be fairly represented by simply including a P, R, and a ''Q-like'' branch, with some enhancement of the intensity of the latter relative to the former two. Based on these premises, the expected shape of the photoionization threshold if only direct ionization were present is illustrated by the thin line at the high-energy side, Fig. 3(a). The simulation was obtained by calculating the positions and intensities of the lines of the representative subbranches, convoluting them with the experimental resolution, and integrating to obtain the ionization probability. Even the direct ionization model predicts that the adiabatic IE is slightly ($\sim$0.004 eV) above the midrise point.

The thicker line in Fig. 3(b) is a model that incorporates rotational autoionization. Converging to every rotational level of the ion, there are Rydberg states that can autoionize if a continuum of the same symmetry, parity, and total angular momentum is available. The rotational structure of the ion suggests that the most likely mechanism for autoionization is the loss of two rotational quanta in the ion core. This reflects the fact that within a given K_a stack every second

TABLE I. Thermochemical values derived in the present work.[a]

Quantity	0 K	298 K
$IE(CH_2)$	10.393 ± 0.011 eV	
$AE(CH_2^+/CH_3)$	15.120 ± 0.006 eV	15.077 ± 0.006 eV
$D_0(H_2C-H)$ to $\tilde{X}\ ^3B_1CH_2$	109.0 ± 0.3 kcal/mol	110.4 ± 0.3 kcal/mol
$D_0(H_2C-H)$ to $\tilde{a}\ ^1A_1CH_2$	118.0 ± 0.3 kcal/mol	119.4 ± 0.3 kcal/mol
$\Delta H_f^{\ominus}(CH_2,\tilde{X}\ ^3B_1)$	93.2 ± 0.3 kcal/mol	93.3 ± 0.3 kcal/mol
$\Delta H_f^{\ominus}(CH_2,\tilde{a}\ ^1A_1)$	102.2 ± 0.3 kcal/mol	102.3 ± 0.3 kcal/mol
$\Delta H_r^{\ominus}[CH_4\rightarrow CH_2(\tilde{X}\ ^3B_1)+H_2]$	109.1 ± 0.3 kcal/mol	111.1 ± 0.3 kcal/mol
$\Delta H_r^{\ominus}[CH_4\rightarrow CH_2(\tilde{a}\ ^1A_1)+H_2]$	118.2 ± 0.3 kcal/mol	120.2 ± 0.3 kcal/mol
$\Delta H_r^{\ominus}[CH_2(\tilde{a}\ ^1A_1)+H_2O\rightarrow CH_3+OH]$	$+0.0\pm0.3$ kcal/mol	-0.0 ± 0.3 kcal/mol
$\Delta H_f^{\ominus}(CH_2^+,\tilde{X}\ ^2A_1)$	332.9 ± 0.2 kcal/mol	333.0 ± 0.2 kcal/mol

[a]Auxiliary values used are: singlet–triplet splitting in CH_2 of 3156 ± 5 $cm^{-1}\equiv9.023\pm0.014$ kcal/mol from Ref. 19; $D_0(H-CH_3)=103.40\pm0.07$ kcal/mol and $\Delta H_{f0}^{\ominus}(CH_3)=35.84\pm0.09$ kcal/mol from Ref. 25; $\Delta H_{f0}^{\ominus}(CH_4)=-15.925\pm0.072$ kcal/mol and $\Delta H_{f0}^{\ominus}(H)=51.6336\pm0.0014$ kcal/mol from Ref. 9; $D_0(HO-H)=118.08\pm0.05$ kcal/mol from Ref. 10; vibrational frequencies of CH_2 and CH_3 for $H_{298}^{\ominus}-H_0^{\ominus}$ from Ref. 33; $H_{298}^{\ominus}-H_0^{\ominus}$ for other species from Refs. 8 and 9.

level possesses the same symmetry properties. Coupling of the angular momentum N with the total spin $S=1$ guarantees that discrete states converging to some level N of the ion have at least one J value in common with continua built upon ionic levels with $N-2$. Hence, about 1/3 of the J space is subject to autoionization by this mechanism. The simulation depicted in Fig. 3(b) includes such autoionization, and predicts that the adiabatic IE is displaced from the midrise point toward higher energy by ~0.008 eV.

Other autoionizing mechanisms, which include $\Delta N=-1$ in conjunction with interactions across different K_a stacks, may also be present. To establish an upper limit to the possible effect of autoionization, the simulation in Fig. 3(c) (thin line at the low-energy side) includes autoionization of *all* energetically appropriate Rydberg states by the $\Delta N=-1$ and -2 mechanisms. This model almost certainly overestimates the overall effect of rotational autoionization, and places the adiabatic IE quite close to the upper end of the threshold shape, ~0.018 eV above the midrise point.

The model described above suggests that the adiabatic IE is almost certainly higher than the midrise of the threshold step, but very likely lower than the upper end of the step, where the plateau commences. Based on such interpretation, and making some allowance for the autoionizing structure in the plateau region, the photoionization measurement presented in Fig. 1 leads to $IE(CH_2)=10.393\pm0.011$ eV. The error bar reflects conservatively the uncertainty in the interpretation of the threshold shape. The value appears to be nominally slightly lower, but otherwise supportive of $IE(CH_2)=10.396\pm0.003$ eV given by Herzberg.[4]

B. Thermodynamical consequences

The photoionization value for the adiabatic IE of triplet methylene, 10.393 ± 0.011 eV is in harmony with Herzberg's extrapolation[4] of 10.396 ± 0.003 eV. While the appearance energy of the CH_2^+ fragment from CH_3 reported here (15.120 ± 0.006 eV at 0 K) is still barely within the error bar of the previous[11] coarser determination (15.09 ± 0.03 eV), its nominal value is $\sim0.03_0$ eV higher. The difference between $AE_0(CH_2^+/CH_3)$ and $IE(CH_2)$ yields directly the bond dissociation energy of the methyl radical, $D_0(H_2C-H)=4.727\pm0.012$ eV$\equiv109.0\pm0.3$ kcal/mol, which becomes 110.4 ± 0.3 kcal/mol at 298 K. Using Herzberg's $IE(CH_2)$ instead of ours, leads to a very similar value of 108.9 ± 0.2 kcal/mol. However, pending further verification of the precise IE of methylene by ZEKE or similar techniques, we choose to retain both the nominal value and the more conservative error bar propagating from our determination of $IE(CH_2)$. The value for $D_0(H_2C-H)$ derived above is ~0.8 kcal/mol higher than what was available previously[10] from the same positive ion cycle.

The C–H bond dissociation energy in methane was recently accurately redetermined[25] as 103.40 ± 0.07 kcal/mol at 0 K. With the well known[9] value of $\Delta H_{f0}^{\ominus}(CH_4)=-15.92_5\pm0.07_2$ kcal/mol, this yields $\Delta H_{f0}^{\ominus}(CH_3)=35.84\pm0.09$ kcal/mol, and, together with $D_0(H_2C-H)$ derived above, produces the best currently available value for $\Delta H_{f0}^{\ominus}(CH_2)=93.2\pm0.3$ kcal/mol (equivalent to 93.3 ± 0.3 kcal/mol at 298 K). Also, the $AE(CH_2^+/CH_3)$ reported here implies $\Delta H_{f0}^{\ominus}(CH_2^+)=332.9\pm0.1$ kcal/mol (333.0 ± 0.3 kcal/mol at 298 K, see Table I).

It is interesting to note that the value of $\Delta H_f^{\ominus}(CH_2)$ derived here is exactly 1 kcal/mol higher than the JANAF recommendation,[8] but in apparently striking agreement (albeit with a considerably tighter error bar) with the selections of Gurvich *et al.*[9] and Wagman *et al.*[7] The present value is in relative harmony with previous experimental determinations,[13,14,17,18,20] especially when the quoted error bars are taken into account. A comparison to theoretical predictions shows excellent agreement with the values by Grev and Schaefer[22] (93.4 ± 0.5 kcal/mol) and Peterson and Dunning[23] (93.1 kcal/mol).

Using the known splitting[19] between $\tilde{a}\ ^1A_1-\tilde{X}\ ^3B_1$ in CH_2 of 3156 ± 5 $cm^{-1}\equiv9.023\pm0.014$ kcal/mol and $\Delta H_{f0}^{\ominus}(CH_2)$ determined above produces $\Delta H_{f0}^{\ominus}(CH_2\tilde{a}\ ^1A_1)=102.2\pm0.3$ kcal/mol (102.3 ± 0.3 kcal/mol at 298 K). Hence, the value of the C–H bond dissociation energy in CH_3 leading to singlet methylene is 118.0 ± 0.3 kcal/mol at 0 K and 119.4 ± 0.3 kcal/mol at 298 K. One of the implications of this inference is that the reaction $CH_2(\tilde{a}\ ^1A_1)$

$+H_2O \rightarrow CH_3+OH$ appears to be essentially thermoneutral, $\Delta H^{\ominus}_{r0}=0.0\pm0.3$ kcal/mol, based on the recently recommended[10] value for $D_0(HO-H)=118.08\pm0.05$ kcal/mol (119.30±0.05 kcal/mol at 298 K). This is to be contrasted with the recently proposed[40] exothermicity of ~2 kcal/mol for this reaction.

V. CONCLUSION

The present paper reports the first direct observation of the ionization threshold region of methylene radical by photoionization. The CH_2 radical has been produced *in situ* by successive hydrogen abstractions with fluorine atoms from methane precursor. The photoionization spectrum displays a prominent steplike ionization onset, which corresponds to the vibrationless $CH_2^+\tilde{X}\ ^2A_1 \leftarrow CH_2\tilde{X}\ ^3B_1$ transition. The extracted adiabatic ionization energy of CH_2 is 10.393±0.011 eV. This is slightly higher than the nominal midrise of the step structure, which is depressed by rotational autoionization effects. The measured ionization energy is in very good agreement with Herzberg's extrapolation of low members ($n=3-6$) of the $nd\ ^3A_2$ Rydberg series.

In a separate set of experiments, the ion yield curve of the CH_2^+ fragment from CH_3 was obtained at room temperature. The fragment appearance energy was determined accurately by fitting as 15.120±0.006 eV at 0 K. Together with IE(CH_2), this experimental measurement provides the best current value for the bond dissociation energy of the methyl radical,
$D_0(H-CH_2)=4.727\pm0.012$ eV=109.0±0.3 kcal/mol (110.4 ±0.3 kcal/mol at 298 K), and implies $\Delta H^{\ominus}_{f0}(CH_2)=93.2$ ±0.3 kcal/mol (93.3±0.3 kcal/mol at 298 K). The latter value makes the reaction $CH_2(\tilde{a}\ ^1A_1)+H_2O \rightarrow CH_3+OH$ essentially thermoneutral, $\Delta H^{\ominus}_{r0}=0.0\pm0.3$ kcal/mol.

ACKNOWLEDGMENT

This work was supported by the U.S. Department of Energy, Office of Basic Energy Sciences, under Contract No. W-31-109-ENG-38.

[1] A. Niehaus, Z. Naturforsch. **22A**, 690 (1967).
[2] W. Reineke and K. Strein, Ber. Bunsenges. Phys. Chem. **80**, 343 (1976).
[3] G. Herzberg, Proc. R. Soc. London, Ser. A **262**, 291 (1961); see also G. Herzberg and J. Shoosmith, Nature (London) **183**, 1801 (1959).
[4] G. Herzberg, Can. J. Phys. **39**, 1511 (1961).
[5] G. Herzberg and J. W. C. Johns, J. Chem. Phys. **54**, 2276 (1971).
[6] (a) D. L. Yeager, J. Chem. Phys. **105**, 8170 (1996); (b) J. A. Nichols, D. Heryadi, D. L. Yeager, and J. T. Golab, *ibid.* **100**, 2947 (1994); (c) N. Russo, E. Sicilia, and M. Toscano, *ibid.* **97**, 5031 (1992); (d) D. Gervy and G. Verhaegen, Int. J. Quantum Chem. **12**, 115 (1977).
[7] D. D. Wagman *et al.*, *The NBS Tables of Chemical Thermodynamic Properties*, NBS Tech. Note No. 270 [J. Phys. Chem. Ref. Data **11**, Suppl. 2 (1982)].
[8] M. W. Chase *et al.*, *JANAF Thermochemical Tables*, 3rd ed. [J. Phys. Chem. Ref. Data **14**, Suppl. 1 (1985)].
[9] (a) L. V. Gurvich, I. V. Veyts, and C. B. Alcock, *Thermodynamic Properties of Individual Substances* (Hemisphere, New York, 1989), Vol. 1, Parts 1 and 2; (b) L. V. Gurvich, I. V. Veyts, and C. B. Alcock, *Thermodynamic Properties of Individual Substances* (Hemisphere, New York, 1991), Vol. 2, Parts 1 and 2.
[10] J. Berkowitz, G. B. Ellison, and D. Gutman, J. Phys. Chem. **98**, 2744 (1994).
[11] W. A. Chupka and C. Lifshitz, J. Chem. Phys. **48**, 1109 (1967).
[12] V. H. Dibeler, M. Krauss, R. M. Reese, and F. Harllee, J. Chem. Phys. **42**, 3791 (1965).
[13] W. A. Chupka, J. Chem. Phys. **48**, 2337 (1968).
[14] K. E. McCulloh and V. H. Dibeler, J. Chem. Phys. **64**, 4445 (1976).
[15] M. Litorja, R. Asher, and B. Ruscic (unpublished).
[16] R. L. Nuttall, A. H. Laufer, and M. V. Kilday, J. Chem. Thermodyn. **3**, 167 (1971).
[17] R. K. Lengel and R. N. Zare, J. Am. Chem. Soc. **100**, 7495 (1978).
[18] D. Feldmann, K. Meier, H. Zacharias, and K. H. Welge, Chem. Phys. Lett. **59**, 171 (1978).
[19] (a) P. R. Bunker, P. Jensen, W. P. Kraemer, and R. Beardsworth, J. Chem. Phys. **85**, 3724 (1986); (b) P. Jensen and P. R. Bunker, *ibid.* **89**, 1327 (1988); (c) D. G. Leopold, K. K. Murray, A. E. Stevens Miller, and W. C. Lineberger, *ibid.* **83**, 4849 (1985).
[20] C. C. Hayden, D. M. Neumark, K. Shobatake, R. K. Sparks, and Y. T. Lee, J. Chem. Phys. **76**, 3607 (1982).
[21] L. A. Curtiss, K. Raghavachari, G. W. Trucks, and J. A. Pople, J. Chem. Phys. **94**, 7221 (1991).
[22] R. S. Grev and H. F. Schaefer III, J. Chem. Phys. **97**, 8389 (1992).
[23] K. A. Peterson and T. H. Dunning, Jr., J. Chem. Phys. **106**, 4119 (1997).
[24] N. L. Doltsinis and P. J. Knowles, J. Chem. Soc., Faraday Trans. **93**, 2025 (1997).
[25] M. Litorja and B. Ruscic, J. Chem. Phys. **107**, 9852 (1997).
[26] (a) B. Ruscic and J. Berkowitz, J. Phys. Chem. **97**, 11451 (1993); (b) J. Chem. Phys. **100**, 4498 (1994); (c) **101**, 7795 (1994); (d) **101**, 7975 (1994); (e) **101**, 10936 (1994); (f) R. L. Asher and B. Ruscic, *ibid.* **106**, 210 (1997); (g) R. L. Asher, E. H. Appelman, and B. Ruscic, *ibid.* **105**, 9781 (1996).
[27] (a) J.-Y. Roncin and F. Launay, *Atlas of the Vacuum Ultraviolet Emission Spectrum of Molecular Hydrogen*, [J. Phys. Chem. Ref. Data Monogr. , 4 (1994)]; (b) R. L. Kelly, *Atomic and Ionic Spectrum Lines Below 2000 Å: Hydrogen Through Krypton*, [J. Phys. Chem. Ref. Data **16**, Suppl. 1 (1987)].
[28] (a) E. Wasserman, W. A. Yager, and V. J. Kuck, Chem. Phys. Lett. **7**, 409 (1970); (b) R. A. Bernheim, H. W. Bernard, P. S. Wang, L. S. Wood, and P. S. Skell, J. Chem. Phys. **53**, 1280 (1970); (c) E. Wasserman, V. J. Kuck, R. S. Hutton, and W. A. Yager, J. Am. Chem. Soc. **92**, 7491 (1970); (d) M. D. Marshall and A. R. W. McKellar, J. Chem. Phys. **85**, 3716 (1986); (e) M. Rosslein, C. M. Gabrys, M.-F. Jagod, and T. Oka, J. Mol. Spectrosc. **153**, 738 (1992); (f) C. F. Bender and H. F. Schaefer III, J. Am. Chem. Soc. **92**, 4984 (1970); (g) C. F. Bender and H. F. Schaefer III, J. Mol. Spectrosc. **37**, 423 (1971); (h) S. V. O'Neil, H. F. Schaefer III, and C. F. Bender, J. Chem. Phys. **55**, 162 (1971); (i) D. R. McLaughlin, C. F. Bender, and H. F. Schaefer III, Theor. Chim. Acta **25**, 352 (1972).
[29] (a) J. Berkowitz, J. P. Greene, H. Cho, and B. Ruscic, J. Chem. Phys. **86**, 1235 (1987). (b) In the analogous case of SiH_2, which appears to be less reactive than CH_2, the singlet and triplet are inverted. In photoionization experiments similar to those presented here, Berkowitz *et al.* [Ref. 29(a)] have observed ionization from the ground singlet state of SiH_2, as well as a rather intense hot band attributable to ionization from the lowest triplet state. Hence the suspicion that wall collisions may not be entirely efficient in electronic relaxation across different multiplicities. In retrospect, rather than attempting to explain the survival mechanism for an enhanced population of the excited triplet, one could simply postulate that the reactive singlet ground state is destroyed by wall collisions more readily than the excited triplet.
[30] F. Westley, D. H. Frizzell, J. T. Herron, R. F. Hampson, and W. G. Mallard, *NIST Chemical Kinetics Database, Ver. 6.0* (NIST Std Ref. Database 17) (USGPO, Washington, DC, 1994).
[31] If both appearance energies have thermodynamical significance, then $AE_0(CH_2^+/CH_4)-AE_0(CH_2^+/CH_3)=D_0(H_3C-H)-D_0(H-H)=4.484$ ±0.003 eV (Ref. 25)—4.4781±0.0001 eV (Ref. 9)=0.006±0.003 eV, since $AE_0(CH_2^+/CH_3)=D_0(H_2C-H)+IE(CH_2)$ and $AE_0(CH_2^+/CH_4)=D_0(H_3C-H)+D_0(H_2C-H)-D_0(H-H)+IE(CH_2)$. The average available internal energy at 298 K of CH_3 is slightly larger ($1.68_1 kT$) than that of CH_4 ($1.54_4\ kT$), and hence $AE_{298}(CH_2^+/CH_4)-AE_{298}(CH_2^+/CH_3)=0.009\pm0.003$ eV. Furthermore, the CH_2^+ fragmentation from CH_4 is subject to delay from ''kinetic shift'' (as discussed in Sec. I), which manifests itself as additional roundness in the threshold region. Thus, when the two onsets are compared in practice, the initial ascending portion of the CH_2^+ fragment yield from CH_4 appears to be displaced toward higher energy by ~0.08 eV, although its slope is such that this gap becomes smaller as the energy increases.

[32] P. C. Haarhoff, Mol. Phys. **7**, 101 (1963).
[33] M. E. Jacox, *Vibrational and Electronic Energy Levels of Polyatomic Transient Molecules*, [J. Phys. Chem. Ref. Data, Monogr. **3** (1994).
[34] The extrapolation leading to IE(CH_2) in Ref. 4 is based on a significantly more limited set of data than in the analogous case of CH_3 (Ref. 3). There, three distinct Rydberg series (two of which had six members each) were identified and used to obtain IE(CH_3). Most members had clearly identifiable and interpretable rotational structure, leading to exact determinations of band origins. Furthermore, there was an even larger body of data on CD_3. The extrapolation led to a spectroscopic value which was slightly ($\sim$0.005 eV) higher than the adiabatic IE(CH_3) [see Ref. 25 and J. A. Blush, P. Chen, R. T. Wiedman, and M. G. White, J. Chem. Phys. **98**, 3557 (1993)]. As opposed to the relative abundance of data on CH_3, a single Rydberg series with only four members is known in CH_2 (Ref. 4). The first member of the series, which usually displays the greatest departure from constant quantum defect, has been interpreted in terms of its rotational structure (Ref. 3), producing a precise value for the band origin. However, the ''first strong band in each group'' had to be used in lieu of band origins (Ref. 4) for the three higher members, where exact determinations are more critical. The paucity of data makes the extrapolated IE value somewhat less convincing than in the case of CH_3. Herzberg recognizes this fact by assigning a substantially larger error bar to IE(CH_2) than to IE(CH_3).
[35] Y. Y. Yamaguchi and H. F. Schaefer III, J. Chem. Phys. **106**, 8753 (1997).
[36] K. K. Irikura and J. W. Hudgens, J. Phys. Chem. **96**, 518 (1997); see also K. K. Irikura, R. D. Johnson III, and J. W. Hudgens, *ibid.* **96**, 6131 (1992).
[37] (a) P. R. Bunker, T. J. Sears, A. R. W. McKellar, K. M. Evenson, and F. J. Lovas, J. Chem. Phys. **79**, 1211 (1983); (b) K. M. Evenson, T. J. Sears, and A. R. W. McKellar, J. Opt. Soc. Am. B **1**, 15 (1984).
[38] M. Rosslein, C. M. Gabrys, M.-F. Jagod, and T. Oka, J. Mol. Spectrosc. **153**, 738 (1992).
[39] (a) G. Herzberg, *Molecular Spectra and Molecular Structure. II. Infrared and Raman Spectra of Polyatomic Molecules* (Krieger, Malabar, FL, 1991); (b) *Molecular Spectra and Molecular Structure. III. Electronic Spectra and Electronic Structure of Polyatomic Molecules* (Krieger, Malabar, FL, 1991).
[40] H. Grotheer, S. Kelm, H. S. T. Driver, R. J. Hutcheon, R. D. Lockett, and G. N. Robertson, Ber. Bunseges. Phys. Chem. **96**, 1360 (1992).